

The construction of second generation wavelet-based multivariable finite elements for multiscale analysis of beam problems

Youming Wang^{*1,2}, Qing Wu¹ and Wenqing Wang¹

¹*School of Automation, Xi'an University of Posts and Telecommunications,
Xi'an 710121, People's Republic of China*

²*State Key Laboratory of Structural Analysis for Industrial Equipment, Dalian University of Technology,
Dalian 116023, P.R. China*

(Received April 30, 2012, Revised January 24, 2014, Accepted March 25, 2014)

Abstract. A design method of second generation wavelet (SGW)-based multivariable finite elements is proposed for static and vibration beam analysis. An important property of SGWs is that they can be custom designed by selecting appropriate lifting coefficients depending on the application. The SGW-based multivariable finite element equations of static and vibration analysis of beam problems with two and three kinds of variables are derived based on the generalized variational principles. Compared to classical finite element method (FEM), the second generation wavelet-based multivariable finite element method (SGW-MFEM) combines the advantages of high approximation performance of the SGW method and independent solution of field functions of the MFEM. A multiscale algorithm for SGW-MFEM is presented to solve structural engineering problems. Numerical examples demonstrate the proposed method is a flexible and accurate method in static and vibration beam analysis.

Keywords: second generation wavelet; multivariable finite element method; generalized variational principles; multiscale structural analysis

1. Introduction

The finite element method (FEM) based on the energy variational principle and discrete interpolation has been an important analysis tool in solving mathematical and engineering problems. Since traditional FEM uses single variable as the nodal values of the independent variable, the rest field functions, such as rotation and moments in the displacement-based FEM, will lose the accuracy for differential or integral operations. The emergence of the MFEM has solved this problem by taking generalized displacement, rotation and moments as independent variables on the basis of generalized potential energy functional. Zhang (1997) established a practical and general constant stress patch test conditions for analyzing and ensuring convergence or robustness of multivariable finite element formulations. Sun (2003) used incompatible multivariable FEM and homogenization theory to model and analyze micromechanical properties

*Corresponding author, Ph.D., E-mail: xautroland@163.com

of braided composite materials. Zhang (2002) presented a perturbed multivariable finite element method with potential for piezoelectric and disturbed surface acoustic waves in plates and layered solids. Since the interpolating basis functions of FEM and MFEM are generally polynomials, a great deal of numerical structural analysis using traditional interpolating basis functions show several disadvantages, i.e., low efficiency, ill-conditioned elements, etc (Zienkiewicz *et al.* 2000, Chen *et al.* 2004).

The adoption of new polynomials or wavelets as interpolating basis functions has recently been a new method to improve the stability and accuracy of traditional FEM. A typical combined method called wavelet-based finite element method incorporates the feature of the multiresolution analysis of wavelet numerical method and discrete approximation of FEM, which has been developed broadly by the mathematicians and engineering researchers in the recent years. He (2012) proposed a new method for the analysis of beam structures using the trigonometric wavelet-based finite elements. Zupan (2009) presented a trigonometric wavelet-based method for the analysis of spatial naturally curved and twisted linear beams based on the linearized finite-strain beam theory. Chen (2004) constructed Daubechies wavelet finite elements for the bending analysis of thin plate with singularities. Xiang (2006, 2007, 2008, 2009) developed a new kind of wavelet-based finite elements using B-spline wavelet on the interval for the analysis of structural problems including beams, plates, shells, shafts, etc. Similarly, the MFEM using new polynomials or wavelets bases has also received much attention. Shen (1992, 1995, 1997) constructed multivariable spline finite elements based on generalized variational principle for the bending analysis of plates and shells. Yu (2010) constructed multivariable finite elements (MFEs) by adopting the Legendre hierarchical polynomials as interpolating basis functions of displacement and generalized force field functions for static and vibration analysis of beams. Han (2005) developed a multivariable wavelet-based FEM based on the Hellinger-Reissner variational principle to resolve the bending problems of thick plates. Zhang (2010) proposed a MFEM based on B-spline wavelet on the interval and the generalized variational principle for thin plate static and vibration analysis. However, the MFEs are generally built for one class of engineering problems and their approximation feature can not be changed after the selection of interpolating functions.

Recently, the introduction of second generation wavelets (SGWs) based on lifting scheme (Sweldens 1996, 1997) eliminates the restriction and deficiency of traditional interpolating functions of MFEM. The lifting scheme provides the users much flexibility to build different SGW bases with prediction and update coefficients for engineering problems depending on the applications. In the last decades, second generation wavelets based on the lifting scheme have gradually been applied in solving various mathematical and engineering problems. Vasilyev *et al.* (Vasilyev *et al.* 2000, 2005, Mehra 2008) established second generation wavelet collocation method to solve partial differential equations (PDE) with general boundary conditions and nonlinearities. Wang *et al.* (2006) developed an adaptive second generation wavelet method to solve wave equations accurately. Pinho *et al.* (2004) discussed a multiresolution analysis for the discretisation of Maxwell equations using second generation wavelets, which reduced the dimensionality and simplified the representation of nonlinear operators. Castrillón-Candás *et al.* (2003) presented spatially adaptive multiwavelets based on the lifting scheme to sparsely represent integral operators on general geometries. He *et al.* (2007) developed a construction method of lifting wavelets to solve field problems with changes in gradients and singularities by designing suitable prediction operators and update operators. Wang *et al.* (2010) constructed a new class of operator-orthogonal wavelets based on the lifting scheme for multiresolution structural analysis.

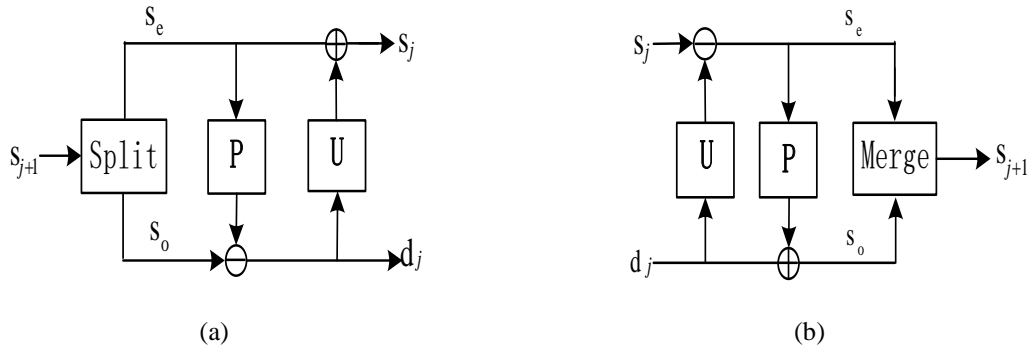


Fig. 1 Second generation wavelet transform (a) decomposition (b) reconstruction

In this paper, a MFEM by adopting SGWs as interpolating functions is proposed for the static and vibration analysis of Euler and Timoshenko beam problems. The organization of the paper: An outline of the paper is as follows. Section 2 introduces the construction of second generation wavelet based on the lifting scheme. Section 3 introduces the computation of connection coefficients. Section 4 discusses the SGW-MFEM for the static and vibration analysis of beam problems based on the generalized variational principles. Section 5 demonstrates the numerical performance of the multiscale SGW-MFEM and conclusions are drawn in Section 6.

2. Second generation wavelets

Lifting scheme (Sweldens 1996, 1997) was presented by Sweldens to custom design second generation wavelets with specific properties, i.e., increasing the vanishing moments, ensuring symmetry and compact support, etc. Generally, the SGW is constructed by steps of split, predict and update shown in Fig. 1.

Let $\mathbf{x} = (x_j)_{j \in \mathbb{Z}}$ be an original signal, the decomposition algorithm of SGW transform is given in the following.

(I) Split: The original signal is divided into even samples s_e and odd samples s_o

$$s_e(k) = x(2k), \quad k \in \mathbb{Z} \tag{1}$$

$$s_o(k) = x(2k + 1), \quad k \in \mathbb{Z} \tag{2}$$

(II) Predict: Using neighboring N even samples s_e to predict odd samples s_o and the prediction difference $d = \{d(k), k \in \mathbb{Z}\}$ is the detail signal after the original signal is decomposed by

$$d(k) = s_o(k) - P(s_e), \quad k \in \mathbb{Z} \tag{3}$$

where $P(N)$ is defined as N point predictor whose prediction coefficients are p_1, p_2, \dots, p_N and N is the predictor order.

(III) Update: Using the obtained N detail signal d to update the even samples s_e and the updated signal $s(k)$ is defined as the approximation signal after the original signal is decomposed

by SGW

$$s(k) = s_e(k) + U(d), \quad k \in Z \quad (4)$$

where $U(N)$ is denoted as N point updater with update coefficients u_1, u_2, \dots, u_N , and N is the updater order.

The reconstruction algorithm of SGW transform includes undo update, undo predict and merge as follows:

(I') Undo update: Approximation signal $s(k)$ and detail signal d can be used to recover even samples $s_e(k)$ of the form

$$s_e(k) = s(k) - U(d), \quad k \in Z \quad (5)$$

(II') Undo predict: Odd samples $s_o(k)$ can be recovered by even samples $s_e(k)$ and detail signal d of the form

$$s_o(k) = d(k) + P(s_e), \quad k \in Z \quad (6)$$

(III') Merge: Original signal can be obtained by using even samples s_e and odd samples s_o

$$x(2k) = s_e(k), \quad k \in Z \quad (7)$$

$$x(2k+1) = s_o(k), \quad k \in Z \quad (8)$$

The lifting scheme provides the users much flexibility to build different SGW bases with prediction and update coefficients for engineering problems depending on the applications. Fig. 2 shows a second generation wavelet with the predictor order $N=4$ and the updater order $N=4$.

3. Connection coefficients of SGW

Since the wavelet numerical method can be viewed as a method in which the approximating function is defined by use of a multiresolution technique, the computation of connection

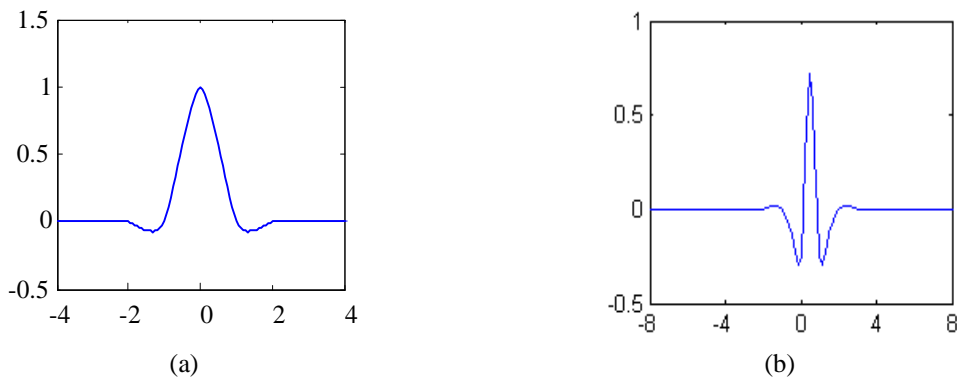


Fig. 2 Second generation wavelet: (a) scaling functions SGW(4) (b) wavelet functions SGW(4,4)

coefficients are based on the multiresolution analysis of the wavelets and scaling functions. While using the scaling functions of SGWs as a test function of finite element method, we would obtain two typical connection coefficients on the interval [0,1] to form stiffness matrices and load vectors (Zienkiewicz *et al.* 2000, Ma *et al.* 2003), such as

$$A_{N,k,l}^{j,a,b} = \int_{-\infty}^{+\infty} \chi_{[0,1]}(\xi) \phi_{j,k}^{(a)} \phi_{j,k}^{(b)} d\xi \tag{9}$$

$$R_{N,k}^{j,c} = \int_{-\infty}^{+\infty} \chi_{[0,1]}(\xi) \xi^c \phi_{j,k} d\xi \tag{10}$$

where $\chi_{[0,1]}(\xi) = \begin{cases} 1 & 0 \leq \xi \leq 1 \\ 0 & \text{otherwise} \end{cases}$. The connection coefficient matrix can be derived as (Wang 2012)

$$(2^{m+n-1}G-I)A_N^{j,m,n} = 0 \tag{11}$$

where G is the coefficient matrix

$$G = \sum_{s,t} (\lambda_{s-2k} \lambda_{t-2l} + \lambda_{s-2k+2^j} \lambda_{t-2l+2^j}) \tag{12}$$

where $-(2N-1) \leq k, l \leq 2^j - 1$ and $\lambda_{j,k,l}$ denote the low-pass filters of SGWs, I is an identity matrix, and $A_N^{j,m,n}$ denotes the $(2^j+2N-1) \times (2^j+2N-1)$ stiffness matrix. Eq. (9) cannot be determined uniquely through the homogeneous Eq. (11), so independent inhomogeneous equations are required for unique solution as

$$\frac{q!}{(q-m)!} \frac{w!}{(w-n)!} \frac{2}{q+w-m-n+1} = 2^{j(m+n)} \sum_{k,l} C_{j,k}^q C_{j,l}^w A_{N,k,l}^{j,m,n} \tag{13}$$

where $C_{j,k}^q = \langle x^q, \phi_{j,k} \rangle$. For the computation of the connection coefficients of load vectors, the multiresolution analysis of SGWs will derive the following equation

$$(2^{m+1}I - B)R_{N,k}^{j,m} = \sum_i \lambda_{i-2k+2^j} \sum_{s=1}^m \binom{m}{s} R_{N,i}^{m-s} \tag{14}$$

where $-(2N-1) \leq k \leq 2^j - 1$, $B = \sum_{i,k} (\lambda_{i-2k} + \lambda_{i-2k+2^j})$.

4. Construction of SGW-MFEM

4.1 Euler beam analysis

4.1.1 Static analysis

Euler beam with two kinds of variables

The boundary and inner nodes in the physical space of multivariable Euler beam element have the degrees of freedom including transverse deflection and moments. Fig. 3 shows the elemental

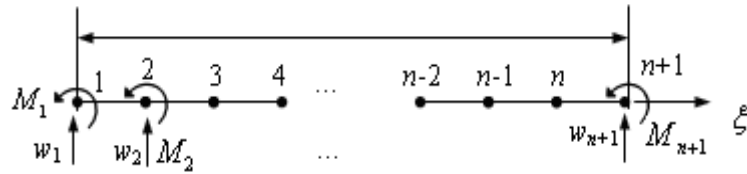


Fig. 3 Euler beam element node array

nodal array in solving domain Ω of the Euler beam. When the second generation wavelets are used to construct the multivariable finite elements, the standard solving domain is divided into $n=2^j+2N$ segments shown in Fig. 3 and the node number is $n+1$. Every node has the degrees of freedom w_i , M_i , $i=1, 2, \dots, n+1$ and the overall number of degrees of freedom is $2(n+1)$.

The generalized potential energy function of the bending problems of an Euler beam with two categories of variables is defined as

$$\Pi_{2p}(w, M) = -\int_0^L M \frac{d^2 w}{dx^2} dx - \int_0^L \frac{M^2}{2EI} dx - \int_0^L q w dx - \sum_i P_i w(x_i) \quad (15)$$

where w is the field deflection function, M the resistance moment field function, E elastic ratio, I cross-section inertia moment, q distributed load.

If the SGW scaling functions are applied to solve Euler beam bending problems, the field functions w and M are interpolated respectively by

$$w(\xi) = \Phi T^e w^e \quad \text{and} \quad M(\xi) = \Phi T^e M^e \quad (16)$$

where $\Phi_1 = \{\phi_{m,-m+1}^j(\xi) \phi_{m,-m+2}^j(\xi) \dots \phi_{m,2^j-1}^j(\xi)\}$ is the one row vector combined by the scaling functions for m at the scale j , the field functions w^e and M^e have the form

$$w^e = \{w_1 \ w_2 \ \dots \ w_{n+1}\}^T, \quad (17)$$

$$M^e = \{M_1 \ M_2 \ \dots \ M_{n+1}\}^T. \quad (18)$$

and T^e is the transformation matrix of the form

$$T^e = ([\Phi^T(\xi_1) \ \Phi^T(\xi_2) \ \dots \ \Phi^T(\xi_{n+1})]^T)^{-1} \quad (19)$$

Substituting Eq. (16) into Eq. (15), according to second kind variation principle

$$\frac{\partial \Pi_{2p}}{\partial M^e} = 0 \quad \text{and} \quad \frac{\partial \Pi_{2p}}{\partial w^e} = 0 \quad (20)$$

we can obtain the second generation wavelet FEM formulations for Euler beam problems

$$\begin{bmatrix} 0 & -\Gamma^{20} \\ -\Gamma^{02} & -\frac{1}{EI} \Gamma^{00} \end{bmatrix} \begin{bmatrix} w^e \\ M^e \end{bmatrix} = \begin{bmatrix} P^e \\ 0 \end{bmatrix} \quad (21)$$

where the integral terms are

$$\Gamma^{00} = (\mathbf{T}^e)^T \{l_e \int_0^1 \Phi^T \Phi d\xi\} (\mathbf{T}^e) \tag{22}$$

$$\Gamma^{20} = (\mathbf{T}^e)^T \left\{ \frac{1}{l_e} \int_0^1 \frac{d^2 \Phi^T}{d\xi^2} \Phi d\xi \right\} (\mathbf{T}^e) \tag{23}$$

$$\Gamma^{02} = (\Gamma^{20})^T \tag{24}$$

the elemental distributed loading column vector is

$$\mathbf{P}^e = (\mathbf{T}^e)^T l_e \int_0^1 q(\xi) \Phi^T d\xi \tag{25}$$

and the lump loading column vector is

$$\mathbf{P}^e = \sum_j P_j (\mathbf{T}^e)^T \Phi^T(\xi_j) \tag{26}$$

Euler beam with three kinds of variables

The generalized potential energy function of the bending problems of an Euler beam with three categories of variables is defined as

$$\Pi_{3p}(w, \sigma, v) = \int_0^L \frac{EIv^2}{2} dx - \int_0^L \sigma v dx + \int_0^L w \frac{d\sigma}{dx} dx - \int_0^L q w dx - \sum_i P_i w(x_i) \tag{27}$$

where w, σ, v are the field deflection function, stress function and strain function, respectively. If the SGW scaling functions are applied to solve Euler beam bending problems, the field functions w, σ and v are interpolated respectively by

$$w(\xi) = \Phi \mathbf{T}^e \mathbf{w}^e \quad \sigma(\xi) = \Phi \mathbf{T}^e \boldsymbol{\sigma}^e \quad v(\xi) = \Phi \mathbf{T}^e \mathbf{v}^e \tag{28}$$

where the field functions w, σ and v have the form

$$\mathbf{w}^e = \{w_1 \ w_2 \ \dots \ w_{n+1}\}^T, \tag{29}$$

$$\boldsymbol{\sigma}^e = \{\sigma_1 \ \sigma_2 \ \dots \ \sigma_{n+1}\}^T, \tag{30}$$

$$\mathbf{v}^e = \{v_1 \ v_2 \ \dots \ v_{n+1}\}^T. \tag{31}$$

Substituting Eq. (28) into Eq. (27), according to second kind variation principle

$$\frac{\partial \Pi_{2p}}{\partial \mathbf{w}^e} = 0, \quad \frac{\partial \Pi_{2p}}{\partial \boldsymbol{\sigma}^e} = 0, \quad \frac{\partial \Pi_{2p}}{\partial \mathbf{v}^e} = 0 \tag{32}$$

we can obtain the second generation wavelet FEM formulations for Euler beam problems

$$\begin{bmatrix} 0 & \Gamma^{10} & 0 \\ \Gamma^{01} & 0 & -\Gamma^{00} \\ 0 & -\Gamma^{00} & EI\Gamma^{00} \end{bmatrix} \begin{bmatrix} \mathbf{w}^e \\ \boldsymbol{\sigma}^e \\ \mathbf{v}^e \end{bmatrix} = \begin{bmatrix} \mathbf{P}^e \\ 0 \\ 0 \end{bmatrix} \tag{33}$$

where the integral terms

$$\Gamma^{10} = (\mathbf{T}^e)^T \left\{ \int_0^1 \frac{d\Phi^T}{d\xi} \Phi d\xi \right\} (\mathbf{T}^e) \quad (34)$$

$$\Gamma^{01} = (\Gamma^{10})^T \quad (35)$$

the elemental distributed loading column vector and the lump loading column vector has the same form as Eqs. (25)-(26).

4.1.2 Vibration analysis

The generalized potential energy function of the eigenvalue problems of a beam with two categories of variables is defined as

$$\Pi_{2p} = - \int_0^L M \frac{d^2 w}{dx^2} dx - \int_0^L \frac{M^2}{2EI} dx - \int_0^L \frac{1}{2} \lambda \rho w^2 dx \quad (36)$$

where w is the field deflection function, M the mass matrix, E elastic ratio, I cross-section inertia moment, ρ is the density, λ is the eigenvalue. When the SGW scaling functions are applied to solve Euler beam eigenvalue problems, the field functions w and M can be interpolated respectively by

$$w(\xi) = \Phi \mathbf{T}^e \mathbf{w}^e \quad \text{and} \quad M(\xi) = \Phi \mathbf{T}^e \mathbf{M}^e \quad (37)$$

Substituting Eq. (37) into Eq. (36), according to second kind variation principle

$$\frac{\partial \Pi_{2p}}{\partial \mathbf{M}^e} = 0 \quad \text{and} \quad \frac{\partial \Pi_{2p}}{\partial \mathbf{w}^e} = 0 \quad (38)$$

we can obtain the second generation wavelet FEM formulations for Euler beam eigenvalue problems

$$\begin{bmatrix} -\frac{1}{EI} \Gamma^{00} & -\Gamma^{02} \\ -\Gamma^{20} & 0 \end{bmatrix} \begin{bmatrix} \mathbf{M}^e \\ \mathbf{w}^e \end{bmatrix} = \begin{bmatrix} 0 & 0 \\ 0 & \lambda \rho \Gamma^{00} \end{bmatrix} \begin{bmatrix} \mathbf{M}^e \\ \mathbf{w}^e \end{bmatrix} \quad (39)$$

where the integral terms are referred to Eq. (22)-(24). The vibration equation of Euler beam has the form

$$|\mathbf{K} - \lambda \mathbf{M}| = 0 \quad (40)$$

4.2 Timoshenko beam analysis

4.2.1 Static analysis

The boundary and inner nodes in the physical space of multivariable Timoshenko beam element have the degrees of freedom including transverse deflection, rotation and moments. When the second generation wavelets are used to construct the multivariable finite elements, the standard solving domain is divided into $n=2^j+2N-1$ segments shown in Fig. 4 and the node number is $n+1$. Every node has the degrees of freedom $w_i, \theta_i, M_i, i=1,2,\dots,n+1$ and the overall number of degrees of freedom is $3(n+1)$.

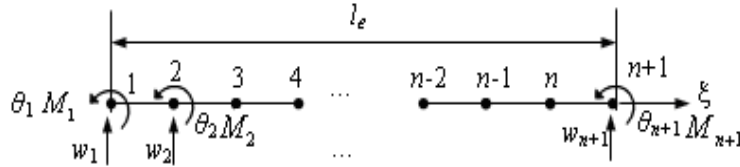


Fig. 4 Timoshenko beam element node array

If the BSWI scaling functions are applied to solve the thick plate bending problems, the field functions of Timoshenko beam are interpolated respectively by

$$w(\xi) = \Phi T^e w^e \tag{41}$$

$$\theta(\xi) = \Phi T^e \theta^e \tag{42}$$

$$M(\xi) = \Phi T^e M^e \tag{43}$$

where $w^e = \{w_1 \ w_2 \ \dots \ w_{n+1}\}^T$, $\theta^e = \{\theta_1 \ \theta_2 \ \dots \ \theta_{n+1}\}^T$, $M^e = \{M_1 \ M_2 \ \dots \ M_{n+1}\}^T$.

The generalized potential energy function of the bending problems of a Timoshenko beam with two categories of variables is defined as

$$\Pi_{2p}(w, \theta, M) = -\int_0^L M \left(\frac{d\theta}{dx}\right) dx + \frac{k_\tau GA}{2} \int_0^L \left(\frac{dw}{dx} - \theta\right)^2 dx - \int_0^L \left(\frac{M^2}{2EI}\right) dx - \int_0^L q w dx \tag{44}$$

where G is sheat modulus, A cross-section, k_τ cross-section shape factor $k_\tau=5/6$ for rectangular cross-section, $k_\tau=9/10$ for circular cross-section.

According to second kind variation principle, let

$$\frac{\partial \Pi_{2p}}{\partial M^e} = 0, \quad \frac{\partial \Pi_{2p}}{\partial \theta^e} = 0 \quad \text{and} \quad \frac{\partial \Pi_{2p}}{\partial w^e} = \mathbf{0} \tag{45}$$

Substituting Eqs. (41),(42),(43) into Eq. (44), we can obtain SGW FEM equations

$$\begin{bmatrix} k_\tau GA \Gamma^{11} & -k_\tau GA \Gamma^{10} & 0 \\ -k_\tau GA \Gamma^{01} & k_\tau GA \Gamma^{00} & -\Gamma^{10} \\ 0 & -\Gamma^{01} & -\frac{1}{EI} \Gamma^{00} \end{bmatrix} \begin{bmatrix} w^e \\ \theta^e \\ M^e \end{bmatrix} = \begin{bmatrix} P^e \\ 0 \\ 0 \end{bmatrix} \tag{46}$$

where the integral form

$$\Gamma^{11} = (T^e)^T \left\{ \frac{1}{l_e} \int_0^1 \frac{d\Phi^T}{d\xi} \frac{d\Phi}{d\xi} d\xi \right\} (T^e) \tag{47}$$

and the element distributed loading column vector and the lump loading column vector has the similar form as Eqs. (25)-(26).

4.2.2 Vibration analysis

The generalized potential energy function of the eigenvalue problems of a Timoshenko beam with two categories of variables is defined as

$$\Pi_{2p}(w, \theta, M) = -\int_0^L \left\{ \frac{EI}{2} \left(\frac{d\theta}{dx} \right)^2 + \frac{k_r GA}{2} \left(\frac{dw}{dx} - \theta \right)^2 \right\} dx - \frac{1}{2} \int_0^L \lambda \rho A w^2 dx - \frac{1}{2} \int_0^L \lambda \rho J \theta^2 dx \quad (48)$$

where J is the inertia moment. If the SGW scaling functions are applied to solve Euler beam eigenvalue problems, the field functions w and M are interpolated respectively by

$$w(\xi) = \Phi \mathbf{T}^e \mathbf{w}^e \quad \text{and} \quad M(\xi) = \Phi \mathbf{T}^e \mathbf{M}^e \quad (49)$$

According to second kind variation principle, let

$$\frac{\partial \Pi_{2p}}{\partial \mathbf{M}^e} = 0 \quad \text{and} \quad \frac{\partial \Pi_{2p}}{\partial \mathbf{w}^e} = \mathbf{0} \quad (50)$$

we can obtain SGW-FEM equations

$$\begin{bmatrix} -\bar{C}\Gamma^{11} & -\bar{C}\Gamma^{10} \\ -\bar{C}\Gamma^{01} & EI\Gamma^{11} + \bar{C}\Gamma^{00} \end{bmatrix} \begin{bmatrix} \mathbf{M}^e \\ \mathbf{w}^e \end{bmatrix} = \begin{bmatrix} \lambda \mathbf{M}_\lambda & 0 \\ 0 & \lambda \bar{\mathbf{M}}_\lambda \end{bmatrix} \begin{bmatrix} \mathbf{M}^e \\ \mathbf{w}^e \end{bmatrix} \quad (51)$$

where

$$\mathbf{M}_\lambda = \rho A \Gamma^{00}, \quad \bar{\mathbf{M}}_\lambda = \rho J \Gamma^{00}, \quad \bar{C} = k_r G t \quad (52)$$

where \mathbf{M}_λ is mass matrix, $\bar{\mathbf{M}}_\lambda$ is the vibration inertia matrix, the vibration equation of Timoshenko beam has the form

$$|\mathbf{K} - \lambda \mathbf{M}| = 0 \quad (53)$$

5. Numerical examples

As the common problem in structural mechanics, Euler and Timoshenko beam problems are calculated by multiscale SGW-MFEM in the following numerical example. The error estimator of second generation wavelet-based multivariable finite element (SGW-MFE) solution is key parameter to test the accuracy of the SGW-MFEM. The error estimator δ_j is chosen to be the uniform norm of the difference e_j between the SGW-MFE solution \bar{u}_j and the exact solution \bar{u}_e respectively in the form

$$\delta_j = \|e_j\|_\infty = \max |\bar{u}_j - \bar{u}_e| \quad (54)$$

To establish a unified standard of error controlling values, the relative error estimate on the level j are defined in the nondimensional form

$$\eta_j = \frac{\|e_j\|_\infty}{\max|\bar{u}_e|} = \frac{\max|\bar{u}_j - \bar{u}_e|}{\max|\bar{u}_e|} \tag{55}$$

The relative error estimation also can indicate the convergence rate of SGW-MFE solution on each level.

Example 1. Fig. 5 shows a rectangle cross-section cantilever beam subjected to distributed loading. The physical parameters are: elastic modulus $E=5 \times 10^{10}$ N/m², shear modulus $G=1.5 \times 10^9$ N/m², width $B=0.625$ m, height $H=1$ m, shear correction coefficient $K_s=5/6$, length $L=10$ m, distributed loading $q(x)=q_0(1-x/L)$, $q_0=10^5$ N, lump force $P_0=5 \times 10^5$ N, moment $M_0=5 \times 10^3$ N·m and the density $\rho=7.9 \times 10^3$ kg/m³, respectively.

A Timoshenko beam model is constructed to solve this problem using SGW-MFEs with order $N=4$ and $N=6$. Table 1 illustrates the error estimator and relative error estimator of beam rotation by multiscale SGW-MFEM, respectively. Table 2 gives the error estimator and relative error estimator of third-order beam eigenvalue by multiscale SGW-MFEM, respectively. It can be observed that the SGW-MFEM converges fast while the scale is increasing. It is noted that the SGW-FEM is referred to the work by Wang (2012) and Ma (2003). Figs. 6 and 7 show the relative error of beam rotation and eigenvalue using multiscale SGW-MFEM with the increasing number

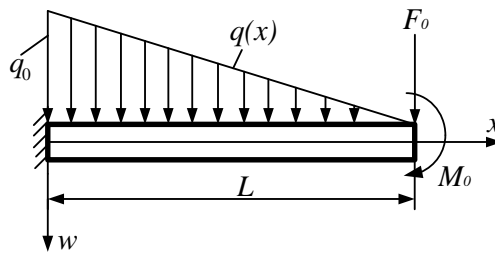


Fig. 5 A cantilever beam subjected to distributed loading

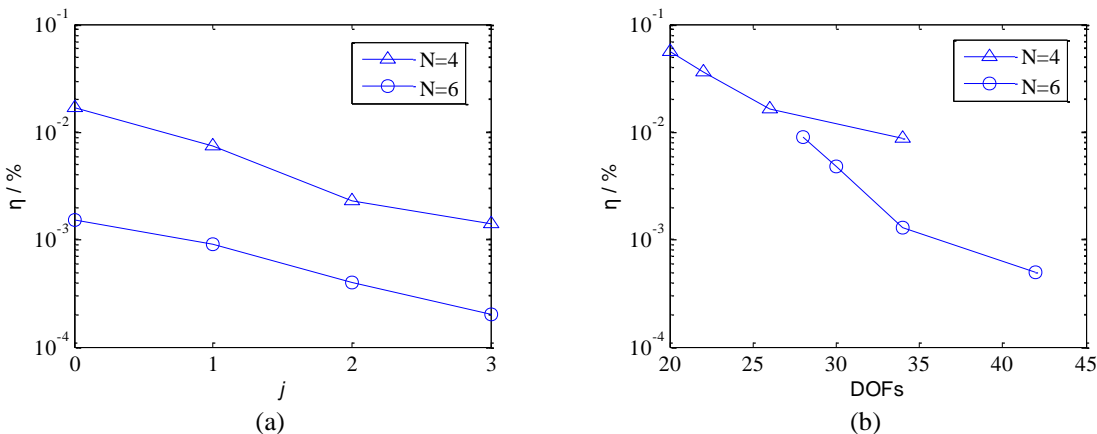


Fig. 6 Convergence of rotation for Timoshenko beam using multiscale SGW-MFEM method with (a) number of levels, (b) degrees of freedom

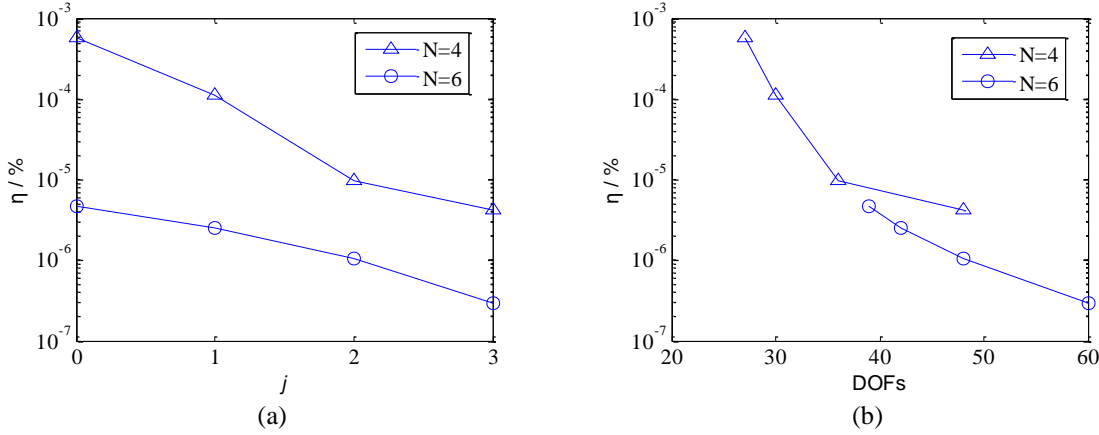


Fig. 7 Convergence of eigenvalue for Timoshenko beam using multiscale SGW-MFEM method with (a) number of levels, (b) degrees of freedom

Table 1 Multiscale rotation solution by SGW-MFEM with order $N=4$ and $N=6$

Space	$N=4$			$N=6$		
	$\delta_j (10^{-5})$	$\eta_j (%)$	DOFs	$\delta_j (10^{-5})$	$\eta_j (%)$	DOFs
V0($j=0$)	16.624	1.67	27	1.519	0.15	39
V1($j=1$)	7.291	0.73	30	0.903	0.09	42
V2($j=2$)	2.255	0.23	36	0.368	0.04	48
V3($j=3$)	1.423	0.14	48	0.156	0.02	60
Cubic FEM	2.541	0.26	82	—	—	—
SGW-FEM	4.217	0.42	32	1.838	0.18	40

Table 2 Third-order eigenvalue solutions by SGW-MFEM with order $N=4$ and $N=6$

Space	$N=4$			$N=6$		
	δ_j	$\eta_j (10^{-4})$	DOFs	δ_j	$\eta_j (10^{-4})$	DOFs
V0($j=0$)	0.021518	5.607	27	0.000176	0.0458	39
V1($j=1$)	0.004289	1.118	30	0.000098	0.0255	42
V2($j=2$)	0.000363	0.095	36	0.000040	0.0105	48
V3($j=3$)	0.000161	0.042	48	0.000012	0.0029	60
Cubic FEM	0.000451	0.117	82	—	—	—
SGW-FEM	0.007716	2.011	32	0.000229	0.0596	40

of levels and degrees of freedoms (DOFs), respectively. It can be seen that numerical solution of the problem using multiscale SGW-MFEM with the order $N=6$ has faster convergence rate and fewer DOFs than the other methods, including SGW-MFEM with the order $N=4$, cubic traditional cubic traditional FEM and SGW-FEM.

Example 2. Fig. 8 shows a simply supported beam with uniform section subjected to a distributed loading $q(x)=q_0x^2e^x$, $q_0=10^3$ N. The physical parameters are: elastic modulus $E=2 \times 10^{11}$ N/m², length $L=10$ m, width $B=0.25$ m, height $H=1$ m and the density $\rho=7.9 \times 10^3$ kg/m³, respectively.

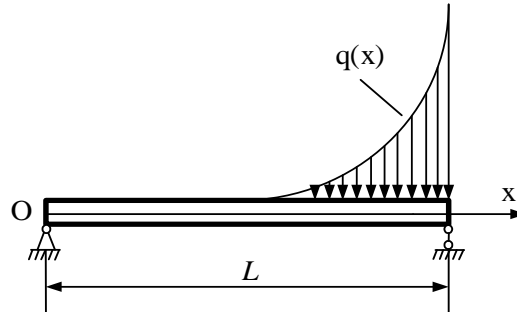


Fig. 8 A simply supported beam subjected to a distributed loading

Table 3 Multiscale moment solution by SGW-MFEM with order $N=4$ and $N=6$

Space	$N=4$			$N=6$		
	$\delta_j (10^7)$	$\eta_j (\%)$	DOFs	$\delta_j (10^7)$	$\eta_j (\%)$	DOFs
V0($j=0$)	5.8629	5.58	20	0.9372	0.89	28
V1($j=1$)	3.7812	3.60	22	0.5087	0.48	30
V2($j=2$)	1.7025	1.62	26	0.1358	0.13	34
V3($j=3$)	0.9166	0.87	34	0.0502	0.05	42
Cubic FEM	1.6983	1.61	62	—	—	—
SGW-FEM	2.0231	1.93	34	0.1108	0.11	42

Table 4 Third-order eigenvalue solutions by SGW-MFEM with order $N=4$

Space	Example 2			Example 3		
	δ_j	$\eta_j (\%)$	DOFs	δ_j	$\eta_j (\%)$	DOFs
V0($j=0$)	0.02126	0.01035	20	0.03251	0.01645	20
V1($j=1$)	0.00832	0.00405	22	0.01573	0.00796	22
V2($j=2$)	0.00138	0.00067	26	0.00271	0.00137	26
V3($j=3$)	0.00031	0.00015	34	0.00049	0.00025	34
Cubic FEM	0.00044	0.00022	82	0.00078	0.00039	82
SGW-FEM	0.00092	0.00045	34	0.00114	0.00057	34

The beam problem can be solved by Euler-Bernoulli model using SGW-MFEM with order $N=4$ and $N=6$. Table 3 shows the error estimator and relative error estimator of beam moment by multiscale SGW-MFEM, respectively. Table 4 illustrates the error estimator and relative error estimator of third-order beam eigenvalue by SGW-MFEM with the order $N=4$, respectively. Fig. 9 shows the relative error of beam moment using multiscale SGW-MFEM with the increasing number of levels and degrees of freedoms, respectively. Numerical results show that the problem using multiscale SGW-MFEM with the order $N=6$ needs fewer degrees of freedom than the other methods to approximate the analytic solution.

Example 3. Fig. 10 shows a rectangle cross-section beam with fixed support subjected to distributed loading. The physical parameters and loading are: elastic modulus $E=10^{11}$ N/m², width $B=0.25$ m, height $H=1$ m, length $L=10$ m, distributed loading $q(x) = q_0 e^{2x} \sin(\pi x / L)$ and $q_0=10^3$ N and the density $\rho=7.9 \times 10^3$ kg/m³, respectively.

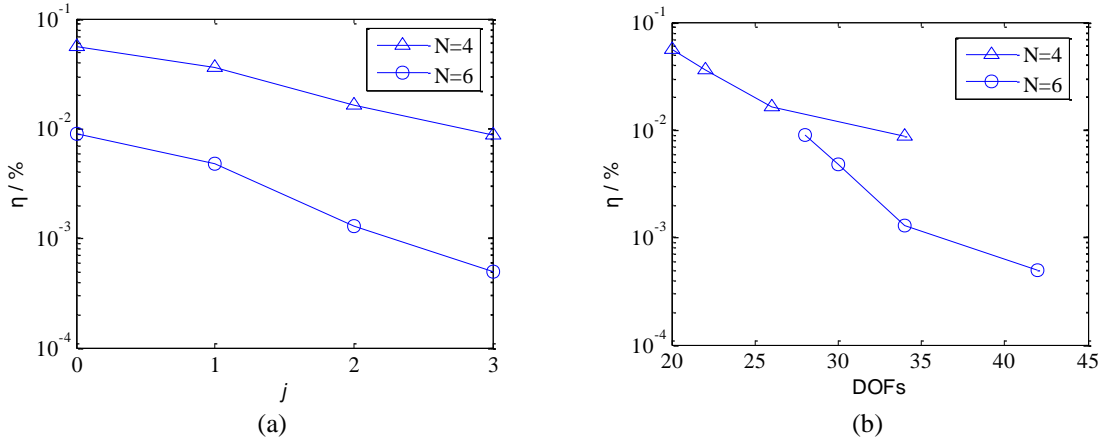


Fig. 9 Convergence of moment for Euler beam using multiscale SGW-MFEM method with (a) number of levels, (b) degrees of freedom

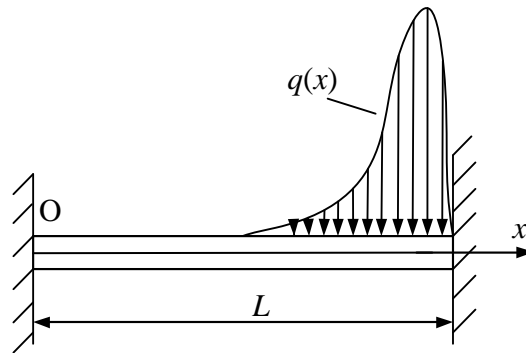


Fig. 10 A fixed supported beam

Table 5 Multiscale deflection solution by SGW-MFEM with order $N=4$ and $N=6$

Space	$N=4$			$N=6$		
	δ_j	η_j (%)	DOFs	δ_j	η_j (%)	DOFs
V0($j=0$)	0.04107	0.3158	30	0.00117	0.0090	42
V1($j=1$)	0.01683	0.1294	33	0.00070	0.0054	45
V2($j=2$)	0.00249	0.0192	39	0.00036	0.0028	51
V3($j=3$)	0.00085	0.0066	51	0.00013	0.0010	63
Cubic FEM	0.00429	0.0330	93	—	—	—
SGW-FEM	0.02528	0.1944	34	0.00351	0.0273	42

Based on the lifting scheme, we can build proper SGWs with order $N=4$ and $N=6$ based on prediction and update coefficient for the Euler-Bernoulli beam analysis. Table 5 gives the error estimator and relative error estimator of third-order beam eigenvalue by multiscale SGW-MFEM with the order $N=4$ and $N=6$, respectively. Table 5 illustrates the error estimator and relative error estimator of beam deflection by multiscale SGW-MFEM with three kinds of variables,

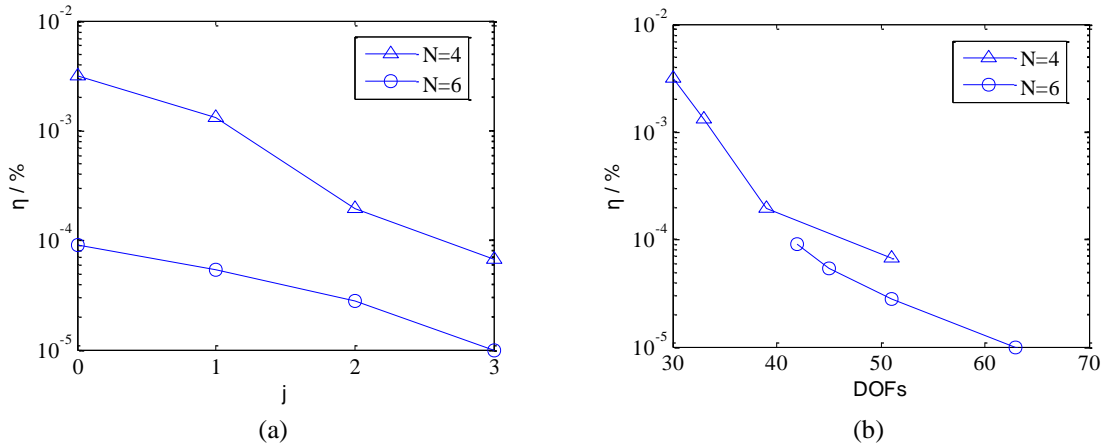


Fig. 11 Convergence of deflection for Euler beam using multiscale SGW-MFEM method with (a) number of levels, (b) degrees of freedom

respectively. Fig. 11 shows the relative error of beam deflection using multiscale SGW-MFEM with the increasing number of levels and degrees of freedoms, respectively. It can be observed that multiscale SGW-MFEM with the order $N=6$ converges fastest in the listed three methods. Therefore, the SGW-MFEM is efficient, accurate and reliable for the solution of beam problems.

6. Conclusions

A multiscale SGW-MFEM is presented for static and vibration beam analysis based on generalized variational principle. The SGW-MFEM is efficient and accurate in the analysis of static and vibration beam analysis because it combines the advantages of custom-design wavelet bases depending on the application by SGW method and the separate interpolation of transverse deflection, rotation and moment by the MFEM. A remarkable property of SGW-MFEM is that it combines the advantages of custom-design wavelet bases depending on the application by SGW method and the separate interpolation of transverse deflection, rotation and moment by the MFEM. Compared to the traditional FEM, the multiscale SGW-MFEM can lead to faster convergent rate in solving structural problems. The numerical examples have shown the effectiveness and validity for the multiscale structural analysis. The extension of SGW-MFEM will be the construction of two- or three- dimensional multivariable finite elements of SGW for the solution of engineering problems.

Acknowledgments

The work in this article is supported by National Natural Science Foundation of China (No. 51205309, 51175097, 61100165), Natural Science Basic Research Plan in Shaanxi Province of China (No. 2013JQ7025) and Open fund of State Key Laboratory of Structural Analysis for Industrial Equipment in Dalian University of Technology (No. GZ1209).

References

- Chen, X.F. and Yang, S.J. (2004), "The construction of wavelet finite element and its application", *Finite Elem. Anal. Des.*, **40**, 541-554.
- Castrillón-Candàs, J. and Amaratunga, K. (2003), "Spatially adapted multiwavelets and sparse representation of integral equations on general geometries", *SIAM J. Sci. Comput.*, **24**(5), 1530-1566.
- Han, J.G., Ren, W.X. and Huang, Y. (2005), "A multivariable wavelet-based finite element method and its application to thick plates", *Finite Elem. Anal. Des.*, **41**, 821-833.
- He, Y.M. and Chen, X.F. (2007), "Adaptive multiresolution finite element method based on second generation wavelets", *Finite Elem. Anal. Des.*, **43**, 566-579.
- He, W.Y. and Ren, W.X. (2012), "Finite element analysis of beam structures based on trigonometric wavelet", *Finite Elem. Anal. Des.*, **51**, 59-66.
- Ma, J.X. and Xue, J.J. (2003), "A study of the construction and application of a Daubechies wavelet-based beam element", *Finite Elem. Anal. Des.*, **39**, 965-975.
- Mehra, M. and Kevlahan, N.K.R. (2008), "An adaptive wavelet collocation method for the solution of partial differential equations on the sphere", *J. Comput. Phys.*, **227**(11), 5610-5632.
- Pinho, P., Ferreira, P.J.S.G. and Pereira, J.R. (2004), "Multiresolution analysis using biorthogonal and interpolating wavelets", *IEEE Anten. Propag. Soc. Symp.*, **2**, 1483-1486.
- Sun, H.Y., Di, S.L. and Zhang, N. (2003), "Micromechanics of braided composites via multivariable FEM", *Comput. Struct.*, **81**(20), 2021-2027.
- Shen, P.C. and Kan, H.B. (1992), "The multivariable spline element analysis for plate bending problems", *Comput. Struct.*, **40**, 1343-1349.
- Shen, P.C. and He, P.X. (1995), "Bending analysis of plates and spherical-shells by multivariable spline element method based on generalized variational principle", *Comput. Struct.*, **55**, 151-157.
- Shen, P.C. and He, P.X. (1997), "Analysis of bending vibration and stability for thin plate on elastic foundation by the multivariable spline element method", *Appl. Math. Mech., English Edition*, **18**, 779-787.
- Sweldens, W. (1997), "The lifting scheme: a construction of second generation wavelets", *SIAM J. Math. Anal.*, **29**(2), 511-546.
- Sweldens, W. (1996), "The lifting scheme: a custom-design construction of biorthogonal wavelets", *Appl. Comput. Harm. Anal.*, **3**(2), 186-200.
- Vasilyev, O.V. and Bowman, C. (2000), "Second generation wavelet collocation method for the solution of partial differential equations", *J. Comput. Phys.*, **165**, 660-693.
- Vasilyev, O.V. and Kevlahan, N.K.R. (2005), "An adaptive multilevel wavelet collocation method for elliptic problems", *J. Comput. Phys.*, **206**, 412-431.
- Wang, Y.B. and Yang, H.Z. (2006), "Second generation wavelet based on adaptive solution of wave equation", *Int. J. Nonlin. Sci. Numer. Simul.*, **7**(4), 435-438.
- Wang, Y.M., Chen, X.F. and He, Y.M. (2010), "New decoupled wavelet bases for multiresolution structural analysis", *Struct. Eng. Mech.*, **35**(2), 175-190.
- Wang, Y.M., Chen, X.F. and He, Z.J. (2012), "A second generation wavelet-based finite element method for the solution of partial differential equations", *Appl. Math. Lett.*, **25**(11), 1608-1613.
- Xiang, J.W., Chen, X.F., He, Y.M. and He, Z.J. (2006), "The construction of plane elastomechanics and Mindlin plate elements of B-spline wavelet on the interval", *Finite Elem. Anal. Des.*, **42**(14-15), 1269-1280.
- Xiang, J.W., Chen, X.F., He, Y.M. and He, Z.J. (2007), "Static and vibration analysis of thin plates by using finite element method of B-spline wavelet on the interval", *Struct. Eng. Mech.*, **25**(5), 613-629.
- Xiang, J.W., Chen, X.F., He, Z.J. and Dong, H.B. (2007), "The construction of 1D wavelet finite elements for structural analysis", *Comput. Mech.*, **40**(2), 325-339.
- Xiang, J.W., Chen, X.F., He, Z.J. and Zhang, Y.H. (2008), "A new wavelet-based thin plate element using B-spline wavelet on the interval", *Comput. Mech.*, **41**(2), 243-255.

- Xiang, J.W., Chen, X.F., Yang, L.F. and He, Z.J. (2008), "A class of wavelet-based flat shell elements using B-spline wavelet on the interval and its applications", *CMES-Comput. Model. Eng. Sci.*, **23**(1), 1-12.
- Xiang, J.W., Chen, X.F. and Yang, L.F. (2009), "Crack identification in short shafts using wavelet-based element and neural networks", *Struct. Eng. Mech.*, **33**(5), 543-560.
- Xiang, J.W., Chen, D.D., Chen, X.F. and He, Z.J. (2009), "A novel wavelet-based finite element method for the analysis of rotor-bearing systems", *Finite Elem. Anal. Des.*, **45**, 908-916.
- Yu, Z.G., Guo, X.L. and Chu, F.L. (2010), "A multivariable hierarchical finite element method for static and vibration analysis of beams", *Finite Elem. Anal. Des.*, **46**, 625-631.
- Zhang, W., Shi, L.Y. and Chen, Y. (2002), "A new perturbed multivariable finite element method with potential for DSAW computation in plates and layered solids", *Commun. Numer. Method. Eng.*, **18**(12), 885-898.
- Zhang, X.W. and Chen, X.F. (2010), "Multivariable finite elements based on B-spline wavelet on the interval for thin plate static and vibration analysis", *Finite Elem. Anal. Des.*, **46**, 416-427.
- Zhang, W. and Chen, D.P. (1997), "The patch test conditions and some multivariable finite element formulations", *Int. J. Numer. Method. Eng.*, **40**(16), 3015-3032.
- Zienkiewicz, O.C. and Taylor, R.L. (2000), *The Finite Element Method*, Butterworth, Heinemann.
- Zupan, E., Zupan, D. and Saje, M. (2009), "The wavelet-based theory of spatial naturally curved and twisted linear beams", *Comput. Mech.*, **43**(5), 675-686.